NUMERICAL MODEL OF PISTON/CYLINDER INTERFACE WITH CONSIDERATION OF TURBULENCE EFFECT FOR WATER HYDRAULICS

Swarnava Mukherjee[1], Haotian Han[1], Lizhi Shang[1*], Georg Herborg[2], Stig Kildegaard Andersen[2]

[1]*Maha Fluid Power Reseach Center, Purdue University, West Lafayette, Indiana 47906*
[2]*Danfoss High Pressure Pumps, Nordborg, Denmark*

* Corresponding author: Tel.: +1 765 496 3174; E-mail address: shangl@purdue.edu

ABSTRACT

Axial piston machines find their use over a wide range of the power spectrum owing to their superior reliability, efficiency, and power density. They are also a key component in applications like reverse osmosis and firefighting wherein the working fluid is water. Utilizing low viscous fluid, such as water, as a working fluid poses challenges in designing the critical lubricating interfaces of the piston pumps. Specifically, low viscosity makes it difficult for the lubricating interfaces to provide sufficient bearing and sealing functions in challenging operating conditions. In order to maintain the lubricating interface performance in water hydraulic piston pumps, costly materials, and tight manufacturing tolerances are often utilized. To improve the efficiency and cost-effectiveness of these pumps, accurate numerical simulation tools that consider the fluid and structure interaction are needed to provide valuable insights into these lubricating interfaces. Although the Reynolds equation is a reliable method for determining the fluid pressure distribution in an oil-based piston pump, it assumes a laminar flow which may not be applicable to water piston machines. For example, in an inclined piston/cylinder interface of a water hydraulic pump, there may be regions in the film wherein the large gap height combined with the low viscosity of water induce turbulence effects. If the traditional Reynolds equation is used in such a scenario, it is likely to overestimate the leakage flow through the interface as it does not account for turbulence. Therefore, it is important to incorporate the effect of turbulence in the diffusive terms of the Reynolds equation to accurately describe the Poiseuille flow with high Reynolds numbers. The challenge is further compounded by the micromotion and deformation of the solid body, resulting in the unevenness of the gap height in the lubricating film. Therefore, the consideration of turbulence can only be applied regionally in such cases. The current study proposes a fluid-structure interaction model with the consideration of the localized turbulent effects. This modeling approach is applied to the piston/cylinder interface of an axial piston machine that uses water as the working fluid. The approach stems from the modification of the Poiseuille term to incorporate a function of the Reynolds number. The fluid dynamics considering the turbulence effect was validated against the solution of the Navier Stokes equation using commercial CFD software. The modified Reynold equation was implemented in an axial piston pump EHL model coupled with the multi-body dynamics. The simulation results from the novel pump model were compared to a measurement and the accuracy of the proposed model was found largely improved from the traditional laminar solution. The calculated flow rate was found to be 54.6% lower with the additional consideration of the turbulence effect in the studied case.

Keywords: Turbulent lubrication, Axial piston machine, Tribology, Experimental validation, Water hydraulics

1. NOMENCLATURE

Symbol	Name	Units
p	Pressure	$[Pa]$
K	Bulk modulus	$[Pa]$
V	Volume	$[m^3]$
ρ	Density	$[kg/m^3]$
$\dot{m}_{in}$	Mass inflow rate	$[kg/s]$
m	Mass	$[kg]$
$\overrightarrow{v_{IF}}$	Inertial frame body velocity	$[m/s]$
$\overrightarrow{F_{l,IF}}$	Inertial frame body force	$[N]$
I_{BF}	Body frame inertia tensor	$[kg \cdot m^2]$
$\overrightarrow{\omega_{BF}}$	Body frame angular velocity	$[rad/s]$
$\overrightarrow{M_{l,BF}}$	Body frame moment	$[N \cdot m]$
ϕ_p	Pressure flow factor	$[-]$
μ	Viscosity	$[Pa \cdot s]$
h	Film thickness	$[m]$
$\overrightarrow{v_m}$	Mean surface velocity	$[m/s]$
ϕ_R	Roughness flow factor	$[-]$
R_q	RMS surface roughness	$[m]$
ϕ_C	Contact flow factor	$[-]$
ϕ_S	Shear flow factor	$[-]$
$\overrightarrow{v_t}$	Bushing velocity	$[m/s]$
$\overrightarrow{v_b}$	Piston velocity	$[m/s]$
$\vec{v}$	Fluid velocity	$[m/s]$
Re	Reynolds number	$[-]$
L_{pist}	Piston length	$[m]$
d_{pist}	Piston diameter	$[m]$
r_{clear}	Nominal radial clearance	$[m]$
L_{bush}	Bushing length	$[m]$
d_{bush}	Bushing diameter	$[m]$

2. INTRODUCTION

Swashplate type axial piston machines are widely used across various industries like agriculture, aerospace, farming and mining equipment, reverse osmosis plants, and firefighting equipment. Their primary advantage is their compactness and efficiency even in demanding operating conditions. Typically, these machines operate with hydraulic oil as the working fluid. However, over the past few years, several researchers have demonstrated the use of water as the working fluid for these machines[1]–[3]. Using water as a working fluid has several advantages: it is sustainable, environmentally friendly, non-flammable, non-toxic, and acts as an effective coolant for the machine. However, water demonstrates certain challenges when used as the working fluid in such machines: its lower viscosity leads to higher leakage flow rates, reduces the load-carrying ability of the lubricating interfaces of the machine, and tends to induce wear in the tribological contacts of the machine. The design of lubricating interfaces of these machines is a critical aspect of designing efficient axial piston machines[4]. Among the three lubricating interfaces of an axial piston machine, the piston/cylinder interface is by far the most critical interface in determining the efficiency and operating limits of the machine[2] owing to its completely hydrodynamic nature. Especially when using water as the working fluid, the design of these interfaces becomes more challenging owing to the physical properties of water. It is therefore crucial to have simulation tools capable of accurately predicting the behavior of the lubricating interfaces to design efficient axial piston machines.

Several modeling approaches for the piston/cylinder lubricating interface of axial piston machines exist in the literature. Wieczorek et al[5] proposed a simulation model for the critical lubricating interfaces of an axial piston machine. Huang et al[6] introduced a fluid-structure interface model for the lubricating interfaces to capture the elasto-hydrodynamic effects. Pelosi et al[7] introduced a fluid structure thermal interaction model to capture thermo-elasto-hydrodynamic effects in the piston/cylinder interface. Ransegnola et al[8] introduced a universal mixed Reynolds equation to capture the cavitated regions of the interface. Mukherjee et al[9] introduced a mutual interaction model between the piston/cylinder gaps to predict distributive fluid behavior in lubrication interfaces. A key limitation in the above-stated simulation models for these lubricating interfaces is that there is no consideration made for localized regions in the interface where the flow might not remain laminar. This is especially important in water hydraulics applications owing to the lower viscosity of water and the possibility of a larger magnitude of wear. Ng and Pan[10] proposed a linearized turbulence theory to account for turbulent regions in lubricating interfaces. This approach was further utilized by Lv et al[11] to model a misaligned journal bearing with mixed lubrication considerations. The current work aims to utilize the linearized turbulence theory to formulate a universal mixed turbulent Reynolds equation tailored for simulating the piston/cylinder interface in axial piston machines.

This paper first describes the modeling approach employed for the piston/cylinder interface operating with water as a working fluid. The turbulent Reynolds equation is introduced to account for localized turbulence effects in the lubricating interface. This is followed by a short comparison of the proposed model with commercial CFD software Simerics MP+ for a simplified geometry. The proposed model is then validated with experimental measurements performed on a reference axial piston machine. Finally, a case study is shown that demonstrates the clearance thresholds at which consideration of turbulence effects becomes important.

3. MODELING APPROACH

The proposed modeling approach for the piston/cylinder interface was developed using a multi-

physics simulation suite, Multics[12]. The base piston/cylinder interface Multics model comprises of several sub-models as shown in **Figure 1**.

The pressure within the displacement chambers, employing a lumped parameter method, serves to provide the boundary conditions for the interface model as well as the forces and moments on the piston. A module dedicated to the dynamics of the piston is employed to solve the equations of motion encompassing all six degrees of freedom for the piston. The resultant piston positions and velocities are subsequently applied to assess the influence of the squeeze and wedge phenomena on the lubricating interface. In this section, a brief description of each of the models is presented.

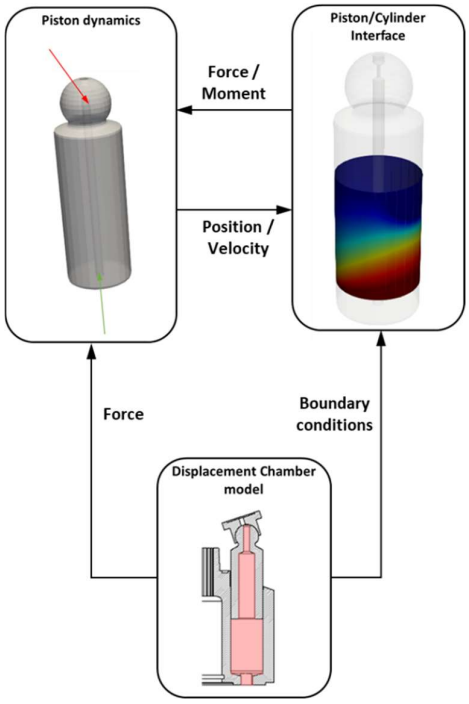

Figure 1: Model Overview

The displacement chamber model solves for the pressure inside a given displacement chamber using the pressure build-up equation as shown in Eq. (1). The volume and volume derivative in Eq. (1) are evaluated using the solution to the piston dynamics equations. $\dot{m}$ in represents the net mass flux into a given displacement chamber. The connection between the displacement chambers and the inlet and outlet ports is assumed to involve orifices with varying areas. These orifice areas represent the momentary flow constriction from a specific displacement chamber to either the outlet or inlet ports. These areas are evaluated using the CFD tool developed by Huang et al[13]. The CFD analysis assesses the smallest instantaneous cross-sectional area along the flow path from the displacement chamber to either of the ports by utilizing 3D representations of the unit. It computes an inviscid flow equation along the flow path and subsequently traces the perpendicular cross-sectional area along the inviscid streamlines to record the minimum cross-sectional area. This assessment is conducted at incremental shaft angles to document the aforementioned variations in the orifice area throughout a complete shaft rotation.

$$\frac{\partial p}{\partial t} = \frac{K}{V}\left(\frac{1}{\rho}\dot{m}_{in} - \frac{\partial V}{\partial t}\right) \tag{1}$$

The forces and moments arising from the pressurized fluid in the displacement chamber and the lubricating interface are used to solve the conservation of linear and angular momentum, as shown in Eq. (2) and (3) respectively, on the piston body. Further details on the force balance of the piston in an axial piston machine can be found in[14].

$$m\frac{d\overrightarrow{v_{IF}}}{dt} = \sum\overrightarrow{F_{\iota,IF}} \tag{2}$$

$$[I_{BF}]\frac{d\overrightarrow{\omega_{BF}}}{dt} = \sum\overrightarrow{M_{\iota,BF}} \tag{3}$$

The Reynolds equation dictates the pressure distribution in a lubricating interface. This pressure distribution is critical to assess the power loss as well as volumetric leakage through the interface. The traditional form of the Reynolds equation is written in terms of the pressure in the lubricating interface as shown by Hamrock et al[15]. This formulation, however, requires the application of the Reynolds boundary condition in the cavitated regions of the interface. This leads to an inaccurate estimation of the flow rate through the interface. In order to alleviate this, Ransegnola[16] proposed a density based formulation of the Reynolds equation. Ransegnola[12] also utilized statistical mixed lubrication relations[17]–[19] to formulate the universal mixed Reynolds equation as shown in Eq. (4).

$$\nabla\cdot\left(\phi_p\left(\frac{Kh^3}{12\mu}\vec{\nabla}\rho\right)\right) = \nabla\cdot\left(\rho\overrightarrow{v_m}\left(\phi_R R_q + \phi_C h\right)\right) + \vec{\nabla}\cdot\left(\rho\frac{\phi_S}{2}R_q(\overrightarrow{v_t} - \overrightarrow{v_b})\right) + \frac{\partial\rho\left(\phi_R R_q + \phi_C h\right)}{\partial t} \tag{4}$$

It is however noted that Eq. (4) is based on the assumption of laminar flow in a lubricating interface. The use of water in axial piston machines combined with the material choices to work with such a low viscous lubricant may lead to wear of the piston and/or bore running surfaces leading to a large gap between the piston and bore. The large gap resulting from the wear coupled with the low viscosity of water leads to the possibility of turbulent flow in the interface geometry, breaking the assumption of laminar flow. Ng and Pan[10] proposed a linearized theory for turbulent lubrication to account for localized turbulent effects in a lubricating interface. This model was also successfully adopted by other researchers[11], [20]. The fundamental idea behind the formulation is the modification of the Poiseuille term in the Reynolds equation as shown in Eq. (5) where $\boldsymbol{Re}$ corresponds to the local Reynolds number in the interface. The combined local Couette and Poiseuille mean velocity in the interface is represented in Eq. (6). As a result, the local Reynolds number in the interface can be expressed as shown in Eq. (7).

$$\nabla\cdot\left(\phi_p\left(\frac{Kh^3}{\boldsymbol{f}(\boldsymbol{Re})\mu}\vec{\nabla}\rho\right)\right) = \nabla\cdot\left(\rho\overrightarrow{v_m}\left(\phi_R R_q + \phi_C h\right)\right) + \vec{\nabla}\cdot\left(\rho\frac{\phi_S}{2}R_q(\overrightarrow{v_t} - \overrightarrow{v_b})\right) + \frac{\partial\rho\left(\phi_R R_q + \phi_C h\right)}{\partial t} \tag{5}$$

$$\vec{v} = \phi_C \overrightarrow{v_m} - \phi_p \frac{h^2}{12\mu} \vec{\nabla} p \tag{6}$$

$$Re = \frac{\rho |\vec{v}| h}{\mu} \tag{7}$$

The function in the Reynolds equation proposed by Ng and Pan[10] is shown in Eq. (8). This variation is graphically represented in **Figure 2**. It is observed that this function has a value close to 12 at low Reynolds numbers recovering the original formulation of the laminar Reynolds equation (4). However, the value of the function increases with the Reynolds number to account for the turbulent effects in the lubricating interface.

$$f(Re) = 12 + 0.00113 Re^{0.9} \tag{8}$$

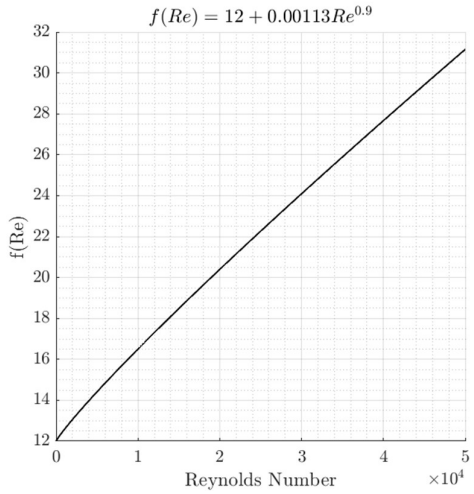

Figure 2: Turbulence Function

In order to assess the validity of the proposed formulation, a simplified thin gap geometry is constructed as shown in **Figure 3** which is representative of a worn piston/cylinder interface of a water hydraulic pump that was studied by the authors' research group. The dimensions in of the simplified geometry are normalized to L_{pist}, d_{pist} and r_{clear}, which correspond to the piston running surface length, piston diameter and nominal radial clearance of the reference unit. The geometry represents a piston tilted inside the bore. The gap height of the simplified geometry is a few times higher than the nominal designed clearance to represent the wear. In order to isolate the pressure driven flow component, a total pressure of 80 bar is specified at the bottom of the geometry and a total pressure of 5 bar is specified at the top of the geometry. No piston motion, body deformation, and thermal effect are considered.

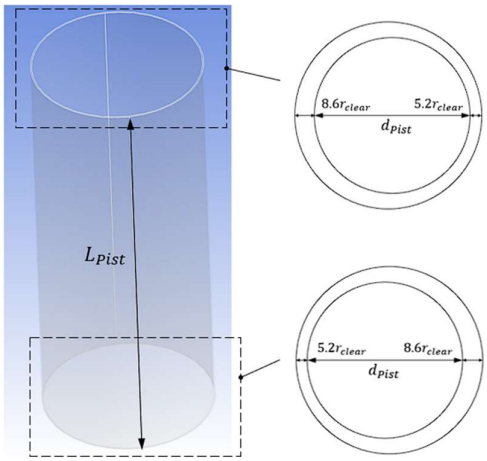

Figure 3: Simple Geometry

Simerics MP+ was used to solve the above-described simplified case with and without a standard $k = \epsilon$ turbulence model. The boundary conditions were specified to be a total pressure of 80 bar on one axial end of the geometry and a total pressure of 5 bar was specified on the other end. The same problem is recreated using the proposed model with Eq. (5) and without Eq. (4) the turbulence factor as well. The boundary conditions for the proposed model were specified pressures of 80 bar and 5 bar at the 2 different axial ends of the geometry. It is also noted that for the model in Simerics MP+, the 5 bar inlet was specified with a fully developed velocity profile. A comparison of the pressure distribution in the fluid geometry is shown in **Figure 4**. It is observed that the pressure distribution prediction demonstrates a significant difference between the laminar and turbulent variants. The distribution predicted by the proposed model closely matches the ones predicted by Simerics MP+.

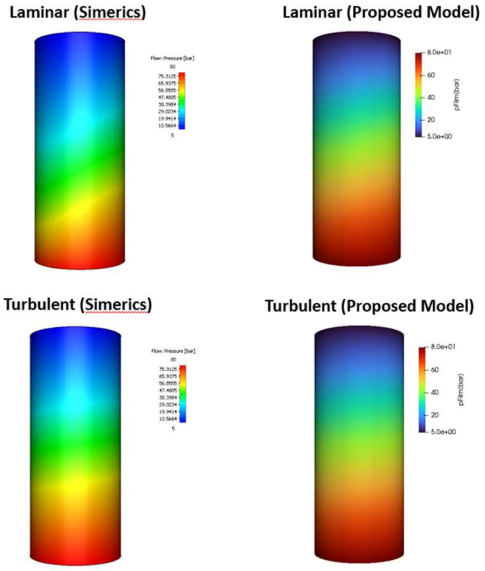

Figure 4: Pressure Distribution Comparison

In order to observe the differences quantitatively, the mass flow rate at the top boundary of the geometry for all the cases is shown in **Figure 5**. Based on the Reynolds number (7) calculation implemented in the proposed model, the turbulence factor multiplier is increased from 0.00113 to 0.00286. It is observed that both the laminar and turbulent mass flow rates predicted by the proposed model and Simerics MP+ match quite well. This match provides confidence in the implementation of the proposed turbulence formulation; however, for a given set of geometry and operating conditions, the turbulence factor may need to be studied further. **Figure 5** presents the prediction of the flow rate with and without the consideration of the turbulence models in both Simerics MP+ and the proposed model by activating and deactivating the turbulence models respectively.

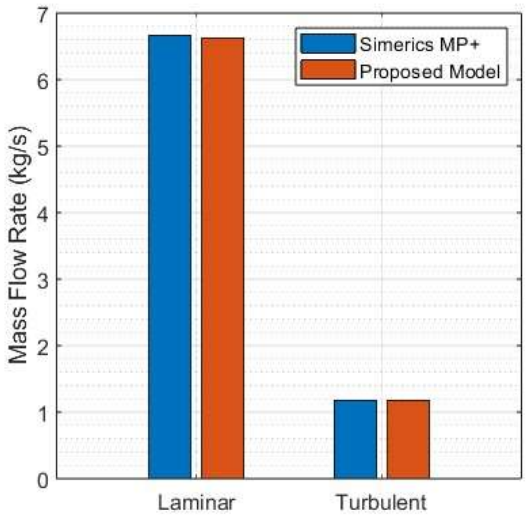

Figure 5: Mass Flow Rate Comparison on Simplified Geometry

4. MODEL VALIDATION

The developed model was validated with experimental measurements performed on the reference fixed displacement swashplate-type water hydraulic pump. The specifications of the reference pump are shown in **Table 1**. Steady-state measurements were performed on the unit according to ISO4409 standards. Steady-state inlet flow rate, outlet flow rate, and a volumetric loss flow rate were measured for the purposes of validation of the proposed model. The highest speed and highest outlet pressure operating conditions were chosen to demonstrate the fidelity of the proposed model. In order to provide a comprehensive insight into the model predictions, steady-state measurements were performed with a set of new unworn bores and a set of severe worn-out bores.

Table 1: Parameters of the reference unit

Parameter	Value [Units]
Displacement	444 [cc/rev]
Maximum speed	1500 [rpm]
Minimum speed	100 [rpm]
Maximum outlet pressure	85 [bar]

Minimum outlet pressure	10 [bar]
Maximum inlet pressure	5 [bar]
Minimum inlet pressure	2 [bar]
Number of pistons	9

In order to incorporate the worn-out bores into the simulation model, the worn-out bores were measured using a contact probe instrument. It is noted here for the reference unit under consideration, insignificant wear was observed on the piston compared to the bore. Thus, for the simulations discussed in the study, the piston wear was neglected. **Figure 6** shows the point cloud that was captured using the contact probe instrument on a worn bore.

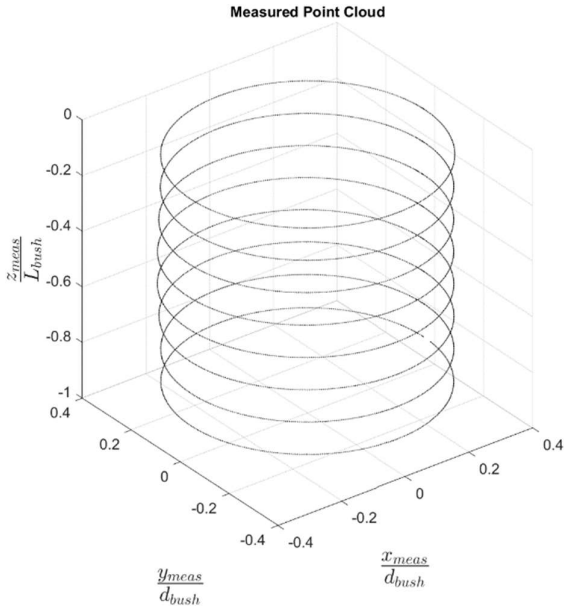

Figure 6: Point Cloud Measurement

The simulation model requires a tabulated input of the wear profile that dictates the variation of the actual profile from the nominal bore diameter. In order to achieve this, a method of the fitted cylinder is utilized to derive the deviation of the measured profile from the nominal bore radius. **Figure 7** shows a representation of the evaluation made to derive the wear profile of a given bore. The geometric centers of each axial layer from **Figure 7** are first evaluated by fitting a circle through these points. A straight three-dimensional line is then fit through these derived centers. A cylinder with a radius of the nominal bore is then constructed about the fitted line. The deviation of each measured point is then evaluated from the resulting fitted cylinder.

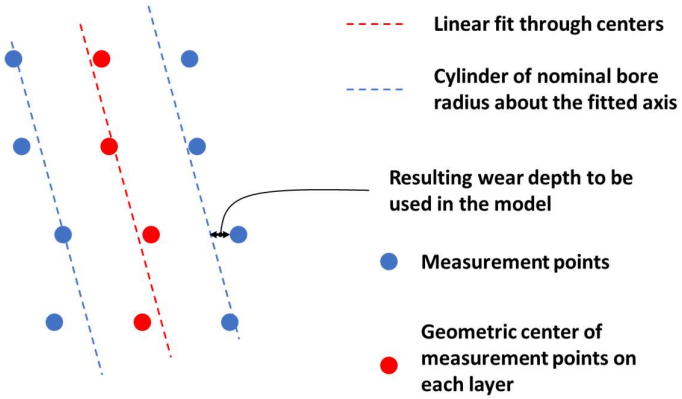

Figure 7: Fitted Cylinder Method to Evaluate Wear Depth

The wear depth distribution on the bore normalized with the nominal radial clearance is shown in **Figure 8**. It is observed that the worn profile demonstrates about 8 times the nominal clearance in some regions. This represents the worst-case wear for such large units with low viscosity working fluids like water. Unlike traditional units with small clearances and high viscosity working fluids, the lubrication flow in these regions of high clearance need not be completely laminar.

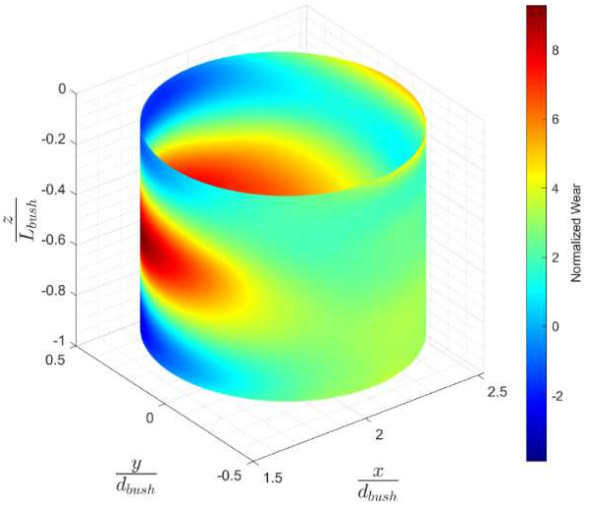

Figure 8: Normalized Bore Wear Profile

The operating condition of interest was chosen to be a differential pressure of 80 bar across the pump at 1500 rpm. Leakages were measured with a set of worn-out bores as well as new unworn bores. The volumetric leakage flow normalized with the theoretical flow rate of the unit is shown in **Table 2**. It is noted here that the experimental setup measured the cumulative leakages from all lubricating interfaces through the drain port on the unit. However, for the purposes of comparison of the experimental measurements with the simulation model of the piston/cylinder interface, the majority of the external leakages were assumed to be rising from the piston/cylinder interface. The simulated leakages discussed in this study are evaluated as the average leakage across all 9 piston/cylinder interfaces of the unit.

Table 2: Measured Leakages

Case	Normalized volumetric leakage flow rate
Unworn bore	0.027
Worn bore	0.106

The simulated variation of the normalized leakage flow through the piston/cylinder interface for the two sets of bores is shown in **Figure 9**. It is observed that for the unworn bore, there is no significant difference between the laminar and turbulent Reynolds equation since the flow is essentially laminar everywhere in the interface. However, for the worn bore, there is a significant difference between the laminar and turbulent Reynolds equations. This is primarily due to the large local clearances in the interface that trigger turbulent flow in the interface. In order to compare the simulated leakages with the experimentally measured ones, an average of the simulated leakages from **Figure 9** over an entire shaft revolution across all 9 piston/cylinder interfaces is performed to provide an estimate of the steady state. In order to evaluate the piston/cylinder interface leakage from the measured volumetric flow loss, it was assumed that the piston/cylinder interface contributes to the majority of the volumetric flow loss. This is because the slipper/swashplate and cylinder block/valveplate interface components are new and therefore provide adequate sealing in their respective interfaces. A comparison between the experimentally evaluated leakages and simulated leakages are shown in **Figure 10**. For the unworn bore, both the models predict the leakage very close to each other because of the low Reynolds number in the unworn gap. The simulation results are expected to be lower than experimentally obtained values since other leakage sources such as slippers and the valveplate are ignored. For the worn bore, it is observed that the turbulent Reynolds equation predicts a leakage much closer to the experimentally measured ones compared to the laminar Reynolds equation. There is however some degree of over-prediction. This is attributed to the coefficients from Eq. (8). Based on Ng and Pan[9], the multiplier and exponent in the turbulence function are specific to geometry and operating conditions.

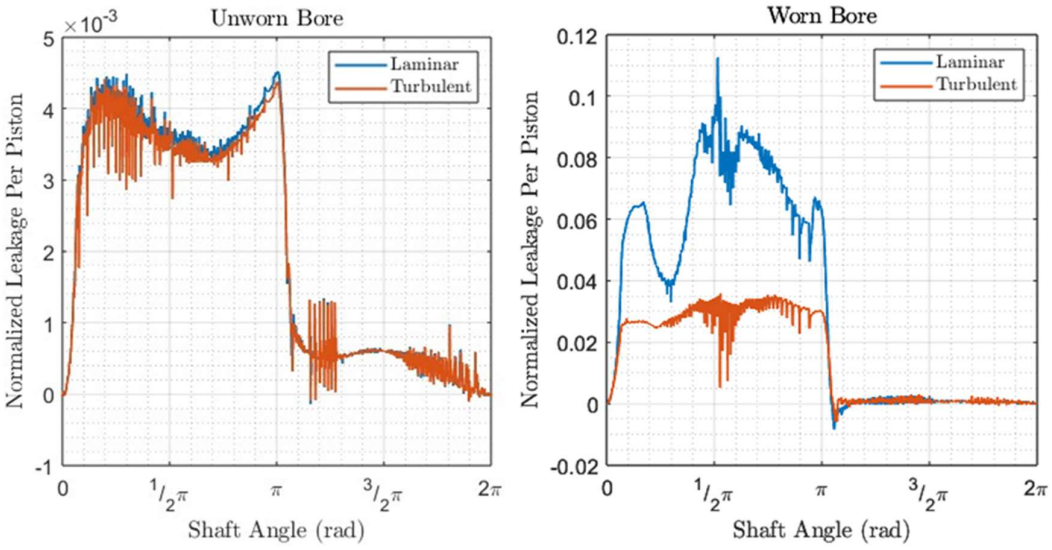

Figure 9: Variation of Leakage from the Piston/Cylinder Interface

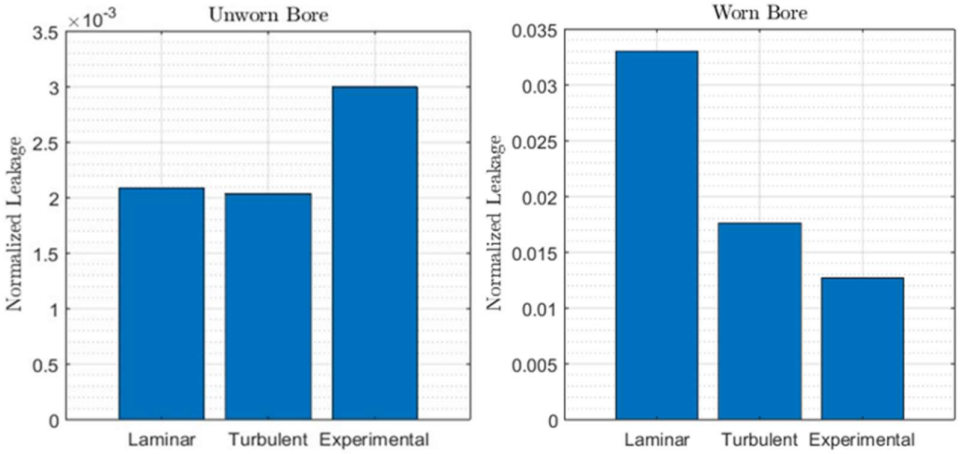

Figure 10: Simulated vs. Experimental Leakage

5. RESULTS AND DISCUSSION

The importance of turbulence in large clearances has been established in the previous section. In order to provide more insight into the applicability of the turbulent Reynolds equation, several cases with partially worn bores have been performed both with the laminar and turbulent Reynolds equations. Table 3 shows the different simulated cases. The 0% wear case corresponds to the nominal bore diameter and the 100% wear case corresponds to the full wear profile from **Figure 8**. The percentages in between correspond to a linearly increasing wear profile between the nominal geometry and fully worn geometry. This study provides insight into a threshold amount of wear after which turbulent effects become non-negligible.

Table 3: Simulation Case Study with Increasing Wear Intensities

Case	% Wear
1	0
2	25
3	50
4	75
5	100

Figure 11 shows the variation of mean leakage between the different cases predicted using the laminar and turbulent Reynolds equations. It is evident that at about 50% wear the prediction between the laminar and turbulent equations deviates indicating that turbulence effects become significant. The larger local clearances combined with the low viscosity of water invalidate the laminar flow assumption locally in the interface.

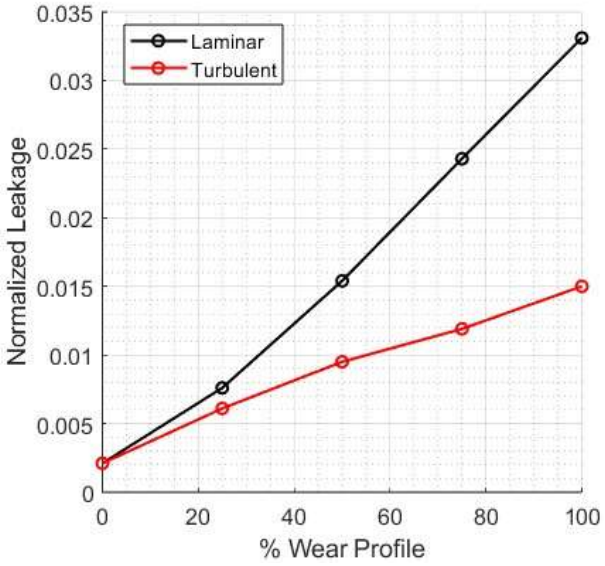

Figure 11: Laminar vs. Turbulent for Varying Clearances

6. CONCLUSION

The study first introduced a framework to incorporate the effect of turbulence in lubricating interfaces. The introduced approach was compared with commercial CFD software, Simerics MP+ for a simplified geometry. Later, the proposed model was validated with experimental measurements on a 444cc/rev commercial axial piston water pump. Finally, a case study was presented to highlight the importance of turbulence effects in lubricating interfaces. The proposed model demonstrates the ability to be used as a predictive tool for extreme operating conditions with innovative geometries and working fluids. Rather than predicting an extremely high leakage rate like the laminar Reynolds equation, the current approach provides a more realistic leakage estimate to avoid false failure metrics during the research and development phase of novel axial piston machines.

REFERENCES

[1] Trostmann E (2000) Tap Water as a Hydraulic Pressure Medium. CRC Press

[2] Ernst M, Vacca A, Ivantysynova M, Enevoldsen G (2020) Tailoring the Bore Surfaces of Water Hydraulic Axial Piston Machines to Piston Tilt and Deformation. Energies, vol. 13, no. 22, Art. no. 22

[3] Ernst M, Ivantysynova M, Vacca A (2022) Shaping the Piston–Cylinder Interfaces of Axial Piston Machines for Running in the High-Pressure Regime with Water as the Hydraulic Fluid. J. Mechanical Engineering Science, vol. 236, no.12, pp. 6851-6872

[4] Hasko D, Shang L, Noppe E, Lefrançois E (2019) Virtual Assessment and Experimental Validation of Power Loss Contributions in Swash Plate Type Axial Piston Pumps. Energies, vol. 12, no. 16, Art. no. 16

[5] Wieczorek U, Ivantysynova M (2002) Computer Aided Optimization of Bearing and Sealing Gaps in Hydrostatic Machines—The Simulation Tool Caspar. Int. J. Fluid Power, vol. 3, no. 1, pp. 7–20

[6] Ivantysynova M, Huang C (2002) Investigation of the Gap Flow in Displacement Machines Considering Elastohydrodynamic Effect. Proc. JFPS Int. Symp. Fluid Power, vol. 2002, no. 5–1, pp. 219–229

[7] Pelosi M, Ivantysynova M (2012) A Geometric Multigrid Solver for the Piston–Cylinder Interface of Axial Piston Machines. Tribol. Trans., vol. 55, no. 2, pp. 163–174

[8] Ransegnola T, Shang L, Vacca A (2022) A study of piston and slipper spin in swashplate type axial piston machines. Tribol. Int., vol. 167, p. 107420

[9] Mukherjee S, Vacca A, Shang L, Sharma A (2023) A Thermal Modeling Approach for the Piston/Cylinder Interface of an Axial Piston Machine Under Asperity Contact. Meccanica, vol. 58, no. 10, pp. 1929-1957

[10] Ng C-W, Pan C H T(1965) A Linearized Turbulent Lubrication Theory. J. Basic Eng., vol. 87, no. 3, pp. 675–682

[11] Lv F, Jiao C, Ta N, Rao Z (2018) Mixed-lubrication analysis of misaligned bearing considering turbulence. Tribol. Int., vol. 119, pp. 19–26

[12] Ransegnola T (2020) A strongly coupled simulation model of positive displacement machines for design and optimization. PhD Dissertation, Purdue University

[13] Ivantysynova M, Huang C, Christiansen S-K (2004) Computer Aided Valve Plate Design - An Effective Way to Reduce Noise. SAE Trans., vol. 113, pp. 162–173

[14] Mukherjee S (2023) A Multi-Domain Thermal Model for Positive Displacement Machines. PhD Dissertation, Purdue University

[15] Hamrock B J, Schmid B J, Jacobson B O (2004) Fundamentals of Fluid Film Lubrication. CRC Press

[16] Ransegnola T, Sadeghi F, Vacca A (2021) An Efficient Cavitation Model for Compressible Fluid Film Bearings. Tribol. Trans., vol. 64, no. 3, pp. 434–453

[17] Patir N, Cheng H S (1978) An Average Flow Model for Determining Effects of Three-Dimensional Roughness on Partial Hydrodynamic Lubrication. J. Lubr. Technol., vol. 100, no. 1, pp. 12–17

[18] Wu C, Zheng L (1989) An Average Reynolds Equation for Partial Film Lubrication With a Contact Factor. J. Tribol., vol. 111, no. 1, pp. 188–191

[19] Patir N, Cheng H S (1979) Application of Average Flow Model to Lubrication Between Rough Sliding Surfaces. J. Lubr. Technol., vol. 101, no. 2, pp. 220–229

[20] Shenoy S B, Pai R (2009) Theoretical investigations on the performance of an externally adjustable fluid-film bearing including misalignment and turbulence effects. Tribol. Int., vol. 42, no. 7, pp. 1088–1100